ELSEVIER

Biophysical Chemistry 86 (2000) 141–153

Biophysical Chemistry

www.elsevier.nl/locate/bpc

Analytical ultracentrifugation and the characterization of chromatin structure ☆

Juan Ausió*

Department of Biochemistry and Microbiology, University of Victoria, Victoria V8W 3P6, British Columbia, Canada

Received 6 January 2000; accepted 16 March 2000

Abstract

This mini review consists of two parts. The first part will provide a brief overview of the theoretical aspects involved in the two kinds of experiments that can be conducted with the analytical ultracentrifuge (sedimentation velocity and sedimentation equilibrium) as they pertain to the study of chromatin. In the following sections, I describe the analytical ultracentrifuge experiments which, in my opinion, have contributed the most to our understanding of chromatin. Few other biophysical techniques, with the exception of X-ray scattering and diffraction, have contributed as extensively as the analytical ultracentrifuge to the characterization of so many different aspects of chromatin structure. In the course of his scientific career, Professor Henryk Eisenberg has made many important contributions to the theoretical aspects underlying ultracentrifuge analysis, especially in the analysis of solutions of polyelectrolytes and biological macromolecules [H. Eisenberg, Biological macromolecules and polyelectrolytes in solution, Clarendon Press, Oxford, 1976]. As an example he has devoted some of his research effort to the characterization of chromatin in solution. This review includes these important contributions.

Keywords: Analytical ultracentrifuge; Sedimentation velocity; Sedimentation equilibrium; Histones; Nucleosome; Chromatin

☆ Dedicated to Heini Eisenberg

* Tel.: +1-250-721 8863; fax: +1-250-7218855.
E-mail address: jausio@uvic.ca (J. Ausió).

0301-4622/00/$ - see front matter
PII: S0301-4622(00)00144-7

1. Theoretical background. A brief overview

1.1. Analytical ultracentrifugation analysis. Transport and the sedimentation equilibrium experiments

The analytical ultracentrifuge allows the characterization of the behavior of macromolecules in solution upon the influence of an ultracentrifugal field. Two basic kinds of experimental approaches can be used: Transport (sedimentation velocity) and equilibrium (sedimentation equilibrium).

In an ideal two component system (consisting of solvent, component 1, and a macromolecule, component 2), the basic general equation for the flow J_2 of the macromolecular component in the ultracentrifuge can be expressed by:

$$J_2 = \underline{\frac{M_2}{Nf_2}\left(\frac{\partial \rho}{\partial C_2}\right)_{\mu}} \omega^2 r C_2 - \underline{\frac{RT}{Nf_2}\left(1 + C_2\frac{\partial \ln y_2}{\partial C_2}\right)} \times \left(\frac{\partial C_2}{\partial r}\right)_t \quad (1)$$

with

$$\left(\frac{\partial \rho}{\partial C_2}\right)_{\mu} = 1 - \bar{v}_2\rho \quad (2)$$

The underlined terms in Eq. (1) can be identified as the sedimentation '*s*' and diffusion '*D*' coefficients.

$$J_2 = s\omega^2 r C_2 - D\left(\frac{\partial C_2}{\partial r}\right)_t \quad (3)$$

diffusion 'D' coefficients.

where C_2 = concentration of macromolecule (component 2) in moles per cubic centimeter; f_2 = frictional coefficient; r = radial distance; M_2 = molecular weight of component 2; N = Avogadro's number; R = gas constant; T = absolute temperature; $\bar{v}_2$ = partial specific volume of component 2; ω = angular speed of the rotor; y_2 = activity coefficient; ρ = solution density.

In sedimentation velocity experiments, the macromolecular solution is subjected to a high centrifugal field (provided by the high angular speed of the rotor) so that the sedimentation flow of macromolecules is very large compared with the diffusion flow. This will create a net flow of component 2 towards the bottom of the cell with the appearance of a moving boundary that can be used to determine the sedimentation coefficient of the macromolecule. As shown by Eq. (2), this parameter is related to the frictional coefficient of the sedimenting molecule and thus provides an extremely sensitive method for determining conformational changes (folding) of macromolecular complexes as a result of changes in the ionic environment.

For an approximately spherical particle,

$$f_2 = 6\pi\eta R_S \quad (4)$$

where R_S = Stokes radius and η = viscosity of the solvent

Thus, if the molecular weight M_2 and the sedimentation coefficient s are known it is possible to estimate the effective molecular radius of the sedimenting macromolecule. In fact, if both the molecular weight M_2 and the partial specific volume v_2 are known it is possible to estimate the radius R_o of an unhydrated sphere corresponding to the volume of the macromolecule

$$R_o = (3M_2\bar{v}_2/4\pi N)^{1/3} \quad (5)$$

with

$$f_o = 6\pi\eta R_o \quad (6)$$

The ratio $f_2/f_o = 1$ for a perfectly spherical molecule and higher values are indicative of the extent of departure from the spherical shape.

In sedimentation equilibrium experiments, the solution is centrifuged at lower angular speeds of the rotor, to create a centrifugal field such that over time, an equilibrium is established in which the net flow $J_2 = 0$ at any point within the cell. Under these conditions, the sedimentation flow and the diffusion flow are balanced at any radial position in the cell (the distance from a point in the cell with respect to the axis of the rotor).

Therefore, Eq. (2) can be rewritten as:

$$\frac{1}{C_2}\frac{\partial C_2}{\partial r} = \frac{M_2\omega^2 r\left(\frac{\partial \rho}{\partial C_2}\right)_\mu}{RT} = 2\frac{\partial \ln C_2}{\partial r^2} \quad (7)$$

which provides the general equation for sedimentation equilibrium analysis.

A more comprehensive description of this section can be obtained from the literature [1–3].

1.2. Analysis of the data

In the case of the sedimentation velocity experiments, several methods have been described to analyze the boundary [4–8].

The method of van Holde and Weischet [6] is particularly useful for the quantitative analysis of multicomponent solutions [7] consisting of a reduced number of sedimenting species. In this method, the moving boundary is divided into a number of equal parts '*i*' each of which correspond to an equal percentile of the boundary (5%, 10% ...). An apparent sedimentation coefficient is then calculated for each fraction [6] using the equation:

$$s_i^{app} = \ln(r_i/r_m)/\omega^2 t \quad (8)$$

where r_m = radial position of the meniscus (equivalent to the position of the boundary at 0 time); r_i = radial position of fraction '*i*'; and t = time at which the boundary was scanned. This analysis is carried out at different time intervals (from which scans for the different boundaries have been collected) and the s_i are plotted as function of $t^{-1/2}$ to yield the 'fan plots' as shown in Fig. 1a. The method has been recently improved [9] to allow the determination of not only the sedimentation coefficient but also the diffusion coefficient of the sedimenting macromolecules and hence their molecular weight [see Eq. (1)], provided that the partial specific volume (υ_2) of the macromolecule(s) being studied is known.

An alternative method developed by Stafford [8] is currently used in the Beckman XL-A analytical ultracentrifuge. This is a modified version of the method described by Schumaker and Schachman [4,5]. In the original method [5], the boundary is divided in '*j*' equally spaced parts along the radial direction so that $(\partial C_2/\partial r)$, and hence $g(s_j)$, at each position can be determined.

$$g(s_j) = \frac{1}{C_2^0}\frac{\partial C}{\partial s} = \frac{(\partial C_2/\partial r)}{C_2^0}\left(\frac{r_j}{r_m}\right)^2 r_j\omega^2 t \quad (9)$$

In this case $g(s_j)$ represents the weight fraction of material sedimenting at s_j, where

$$s_j = \frac{1}{\omega^2}\frac{\partial \ln r_j}{\partial t} \quad (10)$$

As shown by Eq. (7), sedimentation equilibrium provides an absolute method of molecular weight determination provided that the partial specific volume (υ_2) of the macromolecular component is known. However, where the technique becomes most useful is in the determination of the association parameters of multimeric complexes. This stems from the fact that in multiple component systems (containing more than one macromolecular complex) this technique can be used to determine different molecular weight averages (M_n, M_w, M_z, ... M_k) that are characteristic of the composition of these systems. Several methods of analysis have been described to determine these different molecular weight averages from the sedimentation equilibrium data [10–12].

A good example of its usefulness is in the analysis of an ideal two component system consisting of a mixture of two macromolecules (A, B) of molecular weights M_A and M_B and weight fractions $(1-\alpha)$ and α, respectively [13]. In this instance, the following molecular weight averages can be defined:

$$M_n = (1-\alpha)M_A^{-1} + \alpha M_B^{-1} \quad (11)$$

$$M_w = (1-\alpha)M_A + \alpha M_B \quad (12)$$

$$M_z = \frac{(1-\alpha)M_A^2 + \alpha M_B^2}{(1-\alpha)M_A + \alpha M_B} \quad (13)$$

by combining Eqs. (11) and (12) and Eqs. (12) and (13)

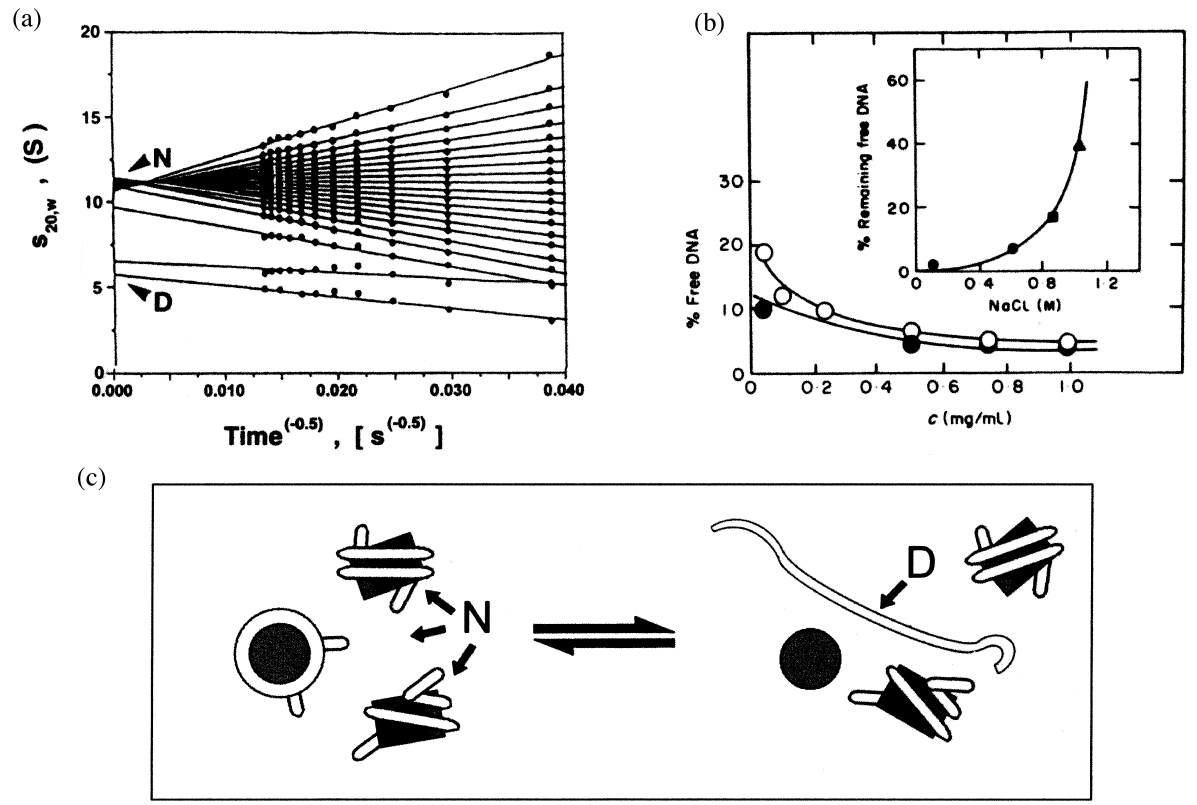

Fig. 1. (a) 'Fan plot' sedimentation velocity analysis of nucleosome core particles from chicken erythrocytes. In this analysis [6], each of the lines converging toward a common $s_{20,w}$ value (in Svedberg units, S) is proportional to the fraction of sample represented (see text for more details). In the plot shown, approximately 90% of the sample sediments as nucleosome core particles (N) ($s_{20,w} = 11.4$ S) and 10% sediments as nucleosomal (146 bp) DNA ($s_{20,w} = 5.4–6$ S). The time units are in seconds. The sedimentation velocity was carried out at 20°C in 100 mM NaCl, 20 mM Tris–HCl, 0.5 mM EDTA (pH 7.5) and 40 000 rev./min. (b) Nucleosome core particles in solution can reversibly dissociate into their constitutive core histone and DNA components [34]. This figure shows the sedimentation velocity analysis of dependence of the percentage of (free) dissociated DNA as a function of the starting nucleosome core particle concentration (in mg/ml of DNA) in 0.6 M NaCl at 20°C (○) and at 10°C (●). In addition to NaCl, the buffer also contained 1 mM Tris–HCl, 0.1 mM EDTA (pH 8.1). The amount of free DNA (d) at any given starting concentration of the sample can be determined from the analysis shown in (a). The inset shows the percentage of free DNA (in the limit of high nucleosome core particle concentration) as a function of the NaCl concentration. (●) 0.1 and 0.6 M NaCl (ref.); (□) data from Vassilev et al. [32]; (□) data from Stacks and Schumacher [30]. (c) Schematic representation of the reversible dissociation equilibrium corresponding to the results shown in (b). The dissociation–association equilibrium depends on concentration, ionic strength, pH and temperature [30–34]. [Part b was reproduced from J. Ausió et al., J. Mol. Biol. 176 (1984) 77–104, with permission from Academic Press Inc.]

$$M_w = -M_A M_B M_n^{-1} + M_A + M_B \quad (14)$$

$$M_z = -M_A M_B M_w^{-1} + M_A + M_B \quad (15)$$

and in general:

$$M_k = -M_A M_B M_{k-1}^{-1} + M_A + M_B \quad (16)$$

Thus, a plot of M_k vs. $1/M_{k-1}$ yields a straight line of slope $-M_A$ M_B which intercepts the hyperbola $M_k/M_{k-1} = 1$ at $M_k = M_A$ and M_B and the plot is referred to as the 'two-species plot'. This kind of analysis is very useful for the characterization of associating systems of the type $nA \rightleftarrows A_n$ where the macromolecular component A as-

sociates to form discrete multimeric complexes nA of a defined number of subunits (n). Eq. (16) then becomes:

$$M_k = -nM_A^2 M_{k-1}^{-1} + (n+1)M_A \quad (17)$$

2. The globular nature of basic chromatin subunit

An important turn in the characterization of chromatin structure occurred in the early 1970s, after it was shown that chromatin could be digested by nucleases. Digestion produced discrete fragments consisting of approximately 100–200 bp of DNA [14] and the existence of a repeating substructure was established [15]. However, it was not clear what the conformation of these fragments was or what stoichiometric histone-DNA composition they had.

Early characterization of the nuclease-resistant particles [16,17] with the analytical ultracentrifuge played an important role in the characterization of the most basic subunit of chromatin which we know today as the nucleosome core particle. The 'PS' particles isolated by the group of Ken van Holde and associates [17] had an average sedimentation coefficient of 12 S. They were shown to consist of a weight fraction composition of 1.53 g protein/g of DNA. Based on this composition and using the partial specific volumes of histones and DNA, a partial specific volume $\upsilon_2 = 0.69\ cm^3/g$ was calculated for these particles [16]. The molecular weight of the complex determined by sedimentation equilibrium using this partial specific volume value was found to be 176 000. Also, the molecular weight of the DNA component, as calculated from its sedimentation coefficient (4.9 s) using the empirical equation $s_{20,w} = 0.1345\ M^{0.32}$ [18], was determined to be 72 000. By combining this value with the protein/DNA weight composition, a molecular weight for the complex of 182 000 was determined which was consistent with the sedimentation equilibrium value. Consequently, it was possible to conclude that the 'PS' particles were highly compact nucleoprotein complexes. Using Eqs. (4)–(6) (shown above) in combination with the values just described, it was found that the 'PS' particles had a frictional ratio $f/f_o = 1.1$ which is close to the ratio observed for globular proteins. A Stokes radius of 40 Å was also determined. This result compared very well with the early electron microscopy data which reported a diameter for the particle ranging from 60 to 80 Å [19,20] to 100 Å [21] and provided the first experimental evidence for the globular conformation of the nucleosome.

Further detailed hydrodynamic studies using sedimentation velocity followed this early characterization [22–24] and provided important insight into the plasticity of the nucleosome which results from changes in the ionic strength, pH of the medium and from exposure to different concentrations of urea. These early characterizations were important in establishing the highly dynamic nature of the nucleosome which is now widely accepted.

3. The nucleosome. A dynamic nucleoprotein complex

The recent resolution of the crystallographic structure of the nucleosome [25], has provided extremely valuable structural information and has confirmed what other biophysical characterizations had anticipated. For instance, of all the potential electrostatic interactions that could potentially be established between the histones and the DNA, only a relatively small number are involved in the maintenance of such structure. This is in contrast to other chromosomal nucleoprotein structures such as the nucleoprotamine complexes which are found in the sperm of many vertebrates. In these latter complexes, the arginine-rich protamines are tightly bound to the genomic DNA through extensive electrostatic interactions [26]. In this instance, dissociation of the complex can only take place at high ionic strengths which are unlikely to occur under physiological conditions, or in the presence of chromatin remodeling protein chaperones such as nucleoplasmin. In the case of the nucleosome, the fact that the level of electrostatic interaction is relatively low most likely reflects the highly dynamic nature of a complex which can freely disso-

ciate and reassociate even at ionic strengths below those corresponding to physiological levels. Such dynamic structure most likely stems from the highly dynamic functional demands of the genetic activity it supports (DNA replication, repair, transcription and recombination). In fact, the crystallographic structure which is presently available [25] most likely represents a single snapshot of an otherwise highly dynamic structure [27].

Work with purified nucleosomes has confirmed this and it has been very helpful in understanding some of the aspects involved in this dynamic behavior. Early sedimentation velocity analysis of these particles revealed the existence of two boundaries that were clearly distinguishable at 0.5–0.6 M NaCl [28,29] (see Fig. 1a). It was possible to show that while the fastest sedimenting component is that of the nucleosome complex, the slowest one is free DNA which dissociates from the nucleosome as the ionic strength increases [28]. At 0.1 M NaCl, the slowest boundary has a sedimentation coefficient of 5–6 *S* (146 bp DNA) and the fastest boundary corresponds to an 11.1 ± 0.1 *S* (nucleosome core particle). It has been shown that the ratio of these two boundaries varies with the ionic strength and the concentration of the sample [30–34]. An exhaustive analysis of this phenomenon carried out in the Henryk Eisenberg laboratory [34,35], showed that the amount of free DNA dissociating from the nucleosome increases with increasing the ionic strength and the temperature and decreases with increasing the concentration of the solution (see Fig. 1b). The dissociation was shown to be reversible [34] and it involves the transfer of the dissociating histone octamer to an undissociated nucleosome [30] (see also Fig. 1c). Evidence from the same laboratory using sedimentation velocity analysis had already indicated that at 0.5–0.6 M NaCl nucleosome core particles can bind more than an additional histone octamer with no significant alteration in the external shape and structure [36].

Whether the process of DNA dissociation involves 'unpeeling' from both ends of DNA in the nucleosome [37] or it simply involves an elastic model of octamer dissociation, is still controversial [38–40].

The equilibrium between nucleosomes and free DNA in solution in fact provides the basis for today's widely used 'exchange methods' of nucleosome reconstitution in which a short DNA fragment of defined sequence is mixed with a large excess native nucleosome core particles at 0.7–1.0 M NaCl and then the ionic strength is decreased to lower values [41,42].

4. Fundamental types of histone association in the histone core

Once it was established that the nucleosome had a globular structure in which the DNA was wrapped about the histone proteins, a fundamental question was the organization of this protein core.

Before the discovery of the nucleosome subunit, many studies had already been carried out designed to understand the mode of association between different histones [43]. The analytical ultracentrifuge again played an important role in this structural characterization. (see Fig. 2). Using the method of sedimentation equilibrium analysis described above, and with the help of the 'two-species plots' [13,44] [see Eqs. (11)–(17)] Roark et al. were able to convincingly demonstrate that core histones H3 and H4 can reversibly associate in solution in a concentration-dependent manner to form a tetrameric complex (see Fig. 2b) [45]. Similarly, they were able to show that H2A and H2B can reversibly associate to form a dimer (see Fig. 2a) [46]. The histone H3–H4 tetramer and the histone H2A–H2B dimers are indeed the basic subunits of the nucleosomal protein core.

Further ultracentrifuge analysis using sedimentation equilibrium analysis and chromatographic techniques carried out by Moudrianakis et al. showed that in the presence of 2 M NaCl, the protein core of the nucleosome is a symmetrical octamer consisting of an H3–H4 tetramer and two H2A–H2B dimers [47]. Further sedimentation equilibrium analysis by the same group showed that the assembly of this octamer occurs in two steps [48] (see Fig. 2c,d). We now know from crystallographic data that the conformation of this histone octamer in high salt [49] is virtually

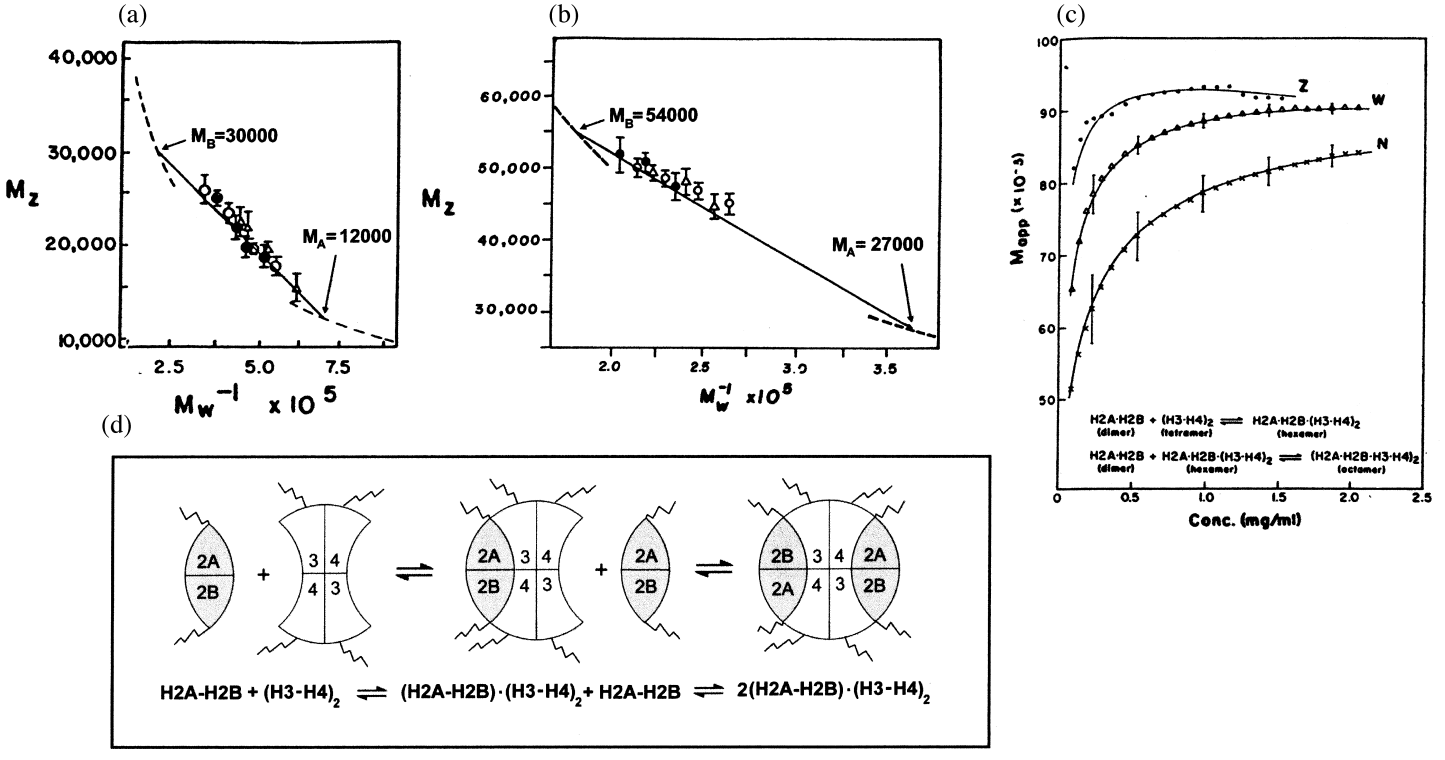

Fig. 2. 'Two-species plot' sedimentation equilibrium analysis of the association behavior for histones H2A–H2B [46] (a) and histones H3–H4 [45] (b). The dashed and solid lines represent the $M_z(1/M_w)$ hyperbola and the two species line, respectively. The values of M_A and M_B (see Eq. (14), are also indicated). The solid line in a corresponds to the equilibrium H2A + H2B Δ H2A − H2B and 2 × (H3–H4) Δ $(H3–H4)_2$ in b. The filled circles,(●); open circles (○) and the triangles (△), correspond to different starting concentrations of the sample. (a) (●) = 0.33 mg/ml; (○) = 0.75 mg/ml; (△) = 1.5 mg/ml. (B) (●) = 0.2 mg/ml; (○) = 0.6 mg/ml; (△) = 1.8 mg/ml. Sedimentation equilibrium experiments were carried out at 20°C in 50 mM NaOAc, 50 mM $NaHSO_3$, 5 mM EDTA, 0.02% NaN_3, pH 5.0 buffer and at 48 000 rev./min (a) and 34 000 rev./min (b). (c) Sedimentation equilibrium analysis of the histone-core complex [48] in 2 M NaCl, 10 mM Tris–HCl pH 7.5 at 20°C at 0.45 mg/ml initial concentration and 26 000 rev./min. Apparent number-average (×), weight (△), and *z*-average (●) are plotted vs. radial solute concentration c_r. The fitted curves are the corresponding apparent averages vs. c_r obeying the hexamer intermediate model shown in d. (d) Sedimentation equilibrium analysis, as shown in (c), in conjunction with gel filtration [47] revealed that the association behavior of the histone H3–H4 tetramer and the histone H2B dimer at high ionic strength proceeds in a two-step mode and leads to the formation of a symmetrical histone octamer which is structurally similar to the histone octamer core of the nucleosome. [Parts a, b and c were, respectively, reproduced from D.E. Roark et al., Biochemistry 15 (1976) 3019–3025; D.E. Roark et al., Biochem. Biophys. Res. Commun. 59 (1974) 542–547; J.E. Godfrey et al., Biochemistry 19 (1980) 1339–1346, with permission from the American Chemical Society and Academic Press Inc.]

identical to that of the histone octamer in the nucleosome [25].

5. Different hierarchies of chromatin folding

As has been stated earlier, the sedimentation coefficient of a macromolecular complex is inversely related to the frictional coefficient and thus sedimentation velocity provides one of the most sensitive and quickest ways to assess the extent and quality of folding and unfolding of macromolecular complexes. The early work of Thomas and Butler [50,51] on the ionic strength dependence of chromatin folding (see Fig. 3a) provides a good example of this. Work from Heini's lab made also a very important contribution in this regard [52–57] and the analytical ultracentrifuge was an important component of this research (see Fig. 3b) [52,53]. It was clear that as the ionic strength of the solution increases from 0 to 100 mM NaCl (or from 0 to 0.4 mM $MgCl_2$) the chromatin fiber undergoes significant compaction (Fig. 3a–c) which reaches a maximum and levels off at approximately physiological ionic strength values [58]. Fig. 3d provides a schematic representation of the different hierarchies of folding of the chromatin fiber as they would correspond to the sedimentation coefficient of the chromatin fiber at low ionic strength in the absence (Fig. 3d1) or in the presence (Fig. 3d3) of linker histones and at higher ionic strength. The model shown in Fig. 3d1,2 was derived from Kirkwood's analysis (see below) of homogeneous reconstituted chromatin fibers [59]. The models shown in Fig. 3d3,4 are an 'idealized' representation of the folding observed by atomic force microscopy [60] and by electron cryomicroscopy [61]. While the ultracentrifuge data can not directly define a particular model, the sedimentation velocity analysis is still very useful support or eliminate the models proposed from experimental analysis obtained with other techniques. An example of this is provided by the recent analysis of the salt-dependent hydrodynamic behavior of native nucleosome dimers [62] the results of which should resolve the long standing issue of whether the linker DNA in the chromatin fiber is bent or straight [60,61,63]. Although the interpretation of these data is still controversial [62,64] there is no doubt that it contains the information that should resolve the linker bendability issue and hence rule out many of the models for the chromatin fiber which have been proposed [65]. In addition, sedimentation velocity analysis has been of enormous value in ascertaining the role(s) played by different histones (i.e. linker histones) and their domains (i.e. N-terminal regions of the core histones) in the folding and maintenance of the physiological state of the chromatin fiber [59,66–69].

Fig. 4b summarizes the different folding hierarchies of the chromatin fiber corresponding to the changes of the sedimentation coefficient shown in Fig. 4a. The increase in the sedimentation coefficient observed as the ionic strength of the medium increases shows that the electrostatic screening of the negatively charged DNA domains from contiguous nucleosomes [70] plays an important role in the folding of the chromatin fiber. The linker histones (histone H1 family) and the *N*-terminal domains ('tails') of the core histones also play an important role in charge shielding [59,66,69] and also provide directionality to the entering and exiting linker DNA regions of the nucleosome thereby increasing the extent and complexity of the folding (see Fig. 4a4–b4). Indeed, histone acetylation (a physiologically relevant post-translational modification which reduces the positive charge of the histone tails) significantly affects the folding o the polynucleosome complexes in the absence of linker histones (see Fig. 4a2–b2) [67].

6. Future perspectives

6.1. Beckman XL-A. A new generation of analytical ultracentrifuge

Long gone are the days when a sudden crash of the diffusion pump or the unexpected failure of the light source in the middle of an ultracentrifuge run would ruin the most important experiment. Also gone are the long hours spent in front

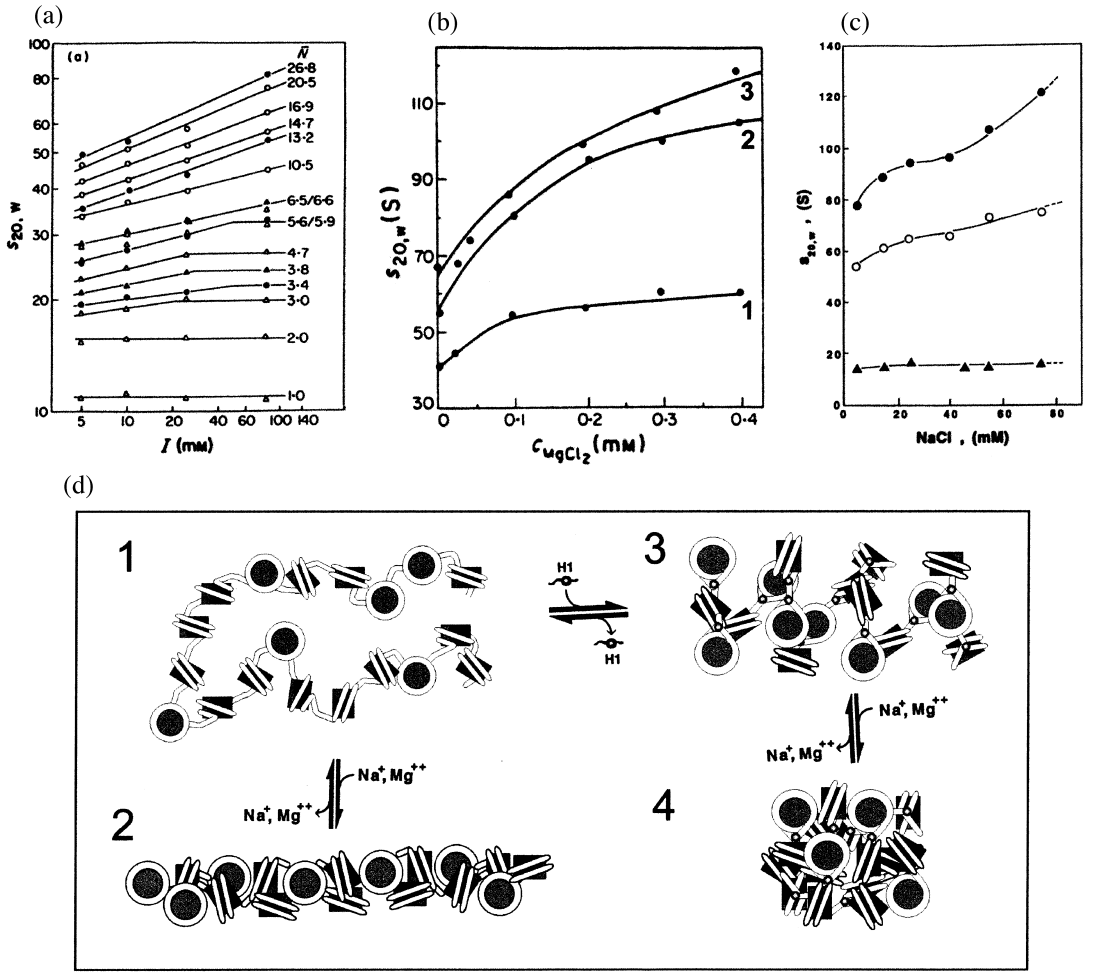

Fig. 3. Sedimentation velocity analysis of chromatin folding. (a) Ionic strength dependence of the sedimentation coefficient $s_{20,w}$ of oligonucleosome fractions [51]. (b) Variation of the sedimentation coefficients $s_{20,w}$ of different oligonucleosome fractions as a function of the $MgCl_2$ concentration [52] of different chromatin fractions [1,($N = 17$); 2, ($N = 35$); 3, ($N = 42$)] in 5 mM NaCl, 1 mM Tris–HCl, (pH 8.0). (c) Salt dependence of the sedimentation coefficient $s_{20,w}$ of native (●); linker-histone stripped (○); and DNA (□); from a chromatin fraction ($N = 43$) in 10 mM Tris–HCl, 0.1 mM EDTA (pH 7.5) [81]. N represents the weight-average number of nucleosomes in chromatin fractions. (d) Schematic representation of the different hierarchies of folding of linker-histone depleted chromatin (1,2) and native chromatin (3,4) at 'low' (1,3) or 'high' concentrations of NaCl and $MgCl_2$. The 'low' and 'high' concentrations refer to the lower and upper values shown in panels (a–c) of this figure. [Parts a, b and c, were, respectively, reproduced from P.J.G. Butler and J.O. Thomas, J. Mol. Biol. 140 (1980) 505–529; J. Ausió et al., J. Mol. Biol. 177 (1984) 373–398; Rabbani et al., J. Biol. Chem. 274 (1999) 18401–18406, with permission from Academic Press Inc. and the American Society for Biochemistry and Molecular Biology.]

of the microcomparator, painstakingly staring with crossed eyes at the interference fringe patterns used for the accurate analysis of sedimentation equilibrium runs which eventually would provide information about different molecular weight averages (M_n, M_w, M_z). With the advent of the Beckman XL-A line of analytical ultracentrifuges a new era in the use of analytical ultracentrifugation analysis has taken place [71,72]. It provides an easier, more reliable and much more versatile piece of equipment in terms of the types of data analysis which can be performed.

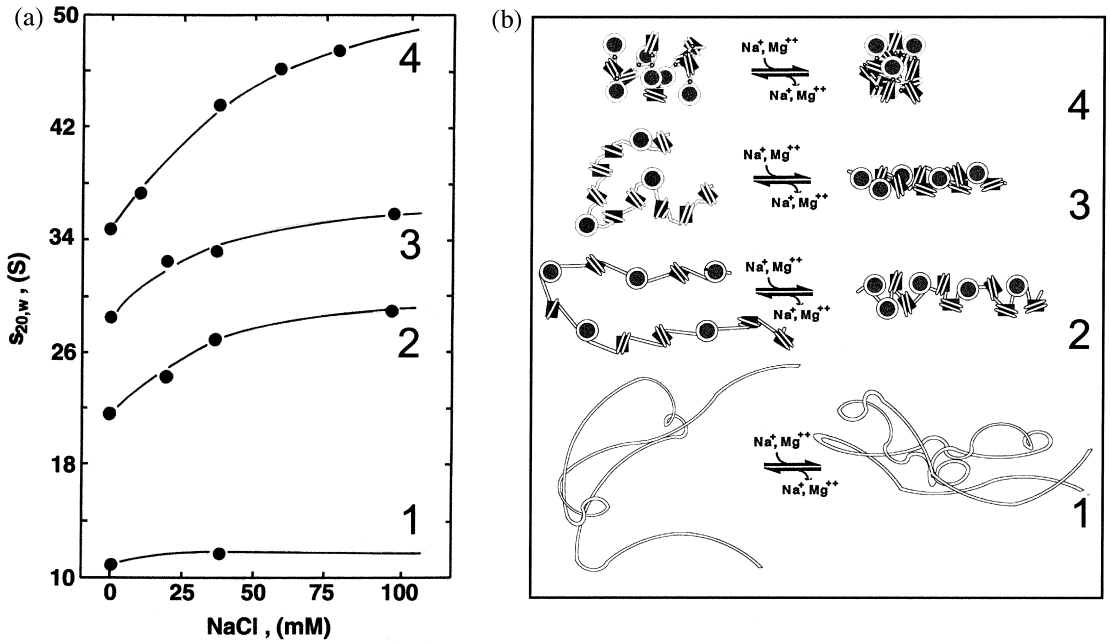

Fig. 4. (a) NaCl dependence of the sedimentation coefficient $s_{20,w}$ of (1): a homogeneous DNA molecule consisting of 12 tandemly arranged copies of a 208 bp fragment of the 5S rRNA gene from the sea urchin *Lytechinus variegatus* [59]; (2) an oligonucleosome complex reconstituted from purified acetylated histone octamers and the same DNA template [67]; (3) a similar oligonucleosome complex reconstituted from non-acetylated core histones [59]; (4) the same complex as in (3) upon further reconstitution with purified histone H1 [77]. Reconstitutions were carried out by salt gradient dialysis [82]. Acetylated core histones were purified from HeLa cell cultures treated with 5 mM sodium butyrate (to inhibit histone deacetylases). Non-acetylated core histones were purified from chicken erythrocytes and histone H1 was purified from non-treated HeLa cell cultures. (b) Schematic representation of the extent of folding of the different complexes analyzed in (a) before (left) and upon increasing the NaCl concentration to 80–100 mM (right).

6.2. Structural characterization of compositionally homogeneous oligonucleosome complexes

In recent years, the structural characterization of chromatin has benefited from the availability of long homogeneous DNA templates designed several years ago by Robert Simpson, which allow the reconstitution of compositionally homogeneous chromatin complexes [73]. These DNA constructs consist of a defined number of tandemly arranged copies of different fragments of the 5 *S* rRNA gene from the sea urchin *Lytechinus variegatus* [73]. The 5 *S* rRNA gene sequence of this organism has a strong positioning signal for the histone octamer and thus allows reconstitution of defined oligonucleosome complexes consisting of approximately equally spaced nucleosomes. One of the most popular templates (208-12) used consists of 12 copies of a 208-bp fragment of this gene. These nucleosome arrays have proven to be very useful as a model for the study of chromatin folding [59,69,74] and their physically homogenous nature makes them amenable to hydrodynamic modeling. In this regard, the use of the Kirkwood formalism [75] for the analysis of the sedimentation velocity coefficient of multimeric complexes using the equation [74,76]:

$$s_n/s_1 = 1 + r/n \sum_i \sum_j (1/R_{ij}) \qquad (18)$$

has been very valuable in distinguishing between (and defining) different folded structures (see Fig. 4).

After several years of failed attempts to successfully reconstitute linker histones onto these complexes, a few methods have been recently described [77,78] that produced homogeneous chromatin complexes which fold in a way which is indistinguishable from that of their native chromatin counterparts. Furthermore, we have recently designed a reconstitution method which allows the reconstitution of chromatin complexes from reversed-phase HPLC purified histones [79,80].

The analytical ultracentrifuge analysis of the chemically and physically homogeneous complexes reconstituted from the 208-12 or other sequence-defined DNA templates in conjunction with well defined fractions of physiologically relevant histone variants and/or their post-translational modifications (such as acetylation, phosphorylation, ubiquitination, or polyribosylation), should provide a unique view on the role played by these epigenetic factors on the processes of chromatin folding. Understanding chromatin folding is a fundamental aspect of understanding gene activity in the eukaryotic cell.

Acknowledgements

I am very grateful to John D. Lewis for his skillful computer assistance with the preparation of the figures and to Susan C. Moore for carefully reading the manuscript. This work was supported by a grant from the Medical Research Council of Canada MT-13104.

References

[1] C. Tanford, Physical Chemistry of Macromolecules, Wiley, New York, 1961.
[2] K.E. van Holde, W.C. Johnson, P.S. Ho, Principles of Physical Biochemistry, Prentice Hall, New York, 1998.
[3] H. Eisenberg, Biological Macromolecules and Polyelectrolytes in Solution, Clarendon Press, Oxford, 1976.
[4] V.N. Schumaker, H.K. Schachman, Ultracentrifugal analysis of dilute solutions, Biochim. Biophys. Acta 23 (1957) 628–639.
[5] H.K. Schachman, Ultracentrifugation in Biochemistry, Academic Press, New York, 1959.
[6] K.E. van Holde, W.O. Weischet, Boundary analysis of sedimentation velocity experiments with monodisperse and paucidisperse solutes, Biopolymers 17 (1978) 1387–1403.
[7] B. Demeler, H. Saber, J.C. Hansen, Identification and interpretation off complexity in sedimentation velocity boundaries, Biophys. J. 72 (1997) 397–401.
[8] W.F. Stafford, III, Boundary analysis in sedimentation transport experiments: a procedure for obtaining sedimentation coefficient distributions using the time derivative of the concentration profile, Anal. Biochem. 203 (1992) 295–301.
[9] B. Demeler, H. Saber, Determination of molecular parameters by fitting sedimentation data to finite-element solutions of the Lamm equation, Biophys. J. 74 (1998) 444–454.
[10] D.A. Yphantis, Equilibrium ultracentrifugation in dilute solutions, Biochemistry 3 (1964) 297–317.
[11] D.C. Teller, T.A. Horbett, E.G. Richards, H.K. Schachman, Ultracentrifuge studies with Rayleigh interference optics. III. Computational methods applied to high-speed sedimentation equilibrium experiments, Ann. N.Y. Acad. Sci. 164 (1970) 66–101.
[12] J.W. Williams, Ultracentrifugation of Macromolecules, Academic Press, New York, 1972.
[13] D.E. Roark, D.A. Yphantis, Studies of self-associating systems by equilibrium ultracentrifugation, Ann. N.Y. Acad. Sci. 164 (1969) 245–278.
[14] R.J. Clark, G. Felsenfeld, Structure of chromatin, Nat. New Biol. 229 (1971) 101–106.
[15] D.R. Hewish, L.A. Burgoyne, Chromatin sub-structure. The digestion of chromatin DNA at regularly spaced sites by a nuclear deoxyribonuclease, Biochem. Biophys. Res. Commun. 52 (1973) 504–510.
[16] R. Rill, K.E. van Holde, Properties of nuclease-resistant fragments of calf thymus chromatin, J. Biol. Chem. 248 (1973) 1080–1083.
[17] C.G. Sahasrabuddhe, K.E. van Holde, The effect of trypsin on nuclease-resistant chromatin fragments, J. Biol. Chem. 249 (1974) 152–156.
[18] A. Prunell, G. Bernardi, Fractionation of native and denatured deoxyribonucleic acid on agarose columns, J. Biol. Chem. 248 (1973) 3433–3440.
[19] A.L. Olins, D.E. Olins, Spheroid chromatin units (ν bodies), J. Cell Biol. 59 (1973) 252a.
[20] A.L. Olins, D.E. Olins, Spheroid chromatin units (ν bodies), Science 183 (1974) 330–332.
[21] C.L.F. Woodcock, Ultrastructure of inactive chromatin, J. Cell Biol. 59 (1973) 368a.
[22] D.E. Olins, P.N. Bryan, R.E. Harrington, W.E. Hill, A.L. Olins, Conformational states of chromatin nu bodies induced by urea, Nucleic Acids Res. 4 (1977) 1911–1931.
[23] V.C. Gordon, V.N. Schumaker, D.E. Olins, C.M. Knobler, J. Horowitz, The temperature and pH dependence of conformational transitions of the chromatin subunit, Nucleic Acids Res. 6 (1979) 3845–3856.
[24] L.J. Libertini, E.W. Small, Salt induced transitions of chromatin core particles studied by tyrosine fluorescence anisotropy, Nucleic Acids Res. 8 (1980) 3517–3534.

[25] K. Luger, A.W. Mäder, R.K. Richmond, D.F. Sargent, T.J. Richmond, Crystal structure of the nucleosome core particle at 2.8 Å resolution, Nature 389 (1997) 251–260.

[26] J.A. Subirana, Proteins as counterions of DNA: a new model of nucleoprotamine structure, in: D. Vasilescu, J. Loz, L. Packer, B. Pullman (Eds.), Advances in Life Sciences, Birkhauser, Basel, 1990, pp. 63–70.

[27] J. Ausió, Crystal structure of the nucleosome core particle at 2.8 Å resolution, Chemtracts 11 (1998) 149–155.

[28] A. Stein, DNA folding by histones: the kinetics of chromatin core particle reassembly and the interaction of nucleosomes with histones, J. Mol. Biol. 130 (1979) 103–134.

[29] H. Eisenberg, G. Felsenfeld, Hydrodynamic studies of the interaction between nucleosome core particles and core histones, J. Mol. Biol. 150 (1981) 537–555.

[30] P.C. Stacks, V.N. Schumaker, Nucleosome dissociation and transfer in concentrated salt solutions, Nucleic Acids Res. 7 (1979) 2457–2467.

[31] R.W. Cotton, B.A. Hamkalo, Nucleosome dissociation at physiological ionic strengths, Nucleic Acids Res. 9 (1981) 445–457.

[32] L. Vassilev, G. Russev, R. Tsanev, Heterogeneity of nucleosomes upon dissociation with salts, Int. J. Biochem. 13 (1981) 1247–1255.

[33] T.D. Yager, K.E. van Holde, Dynamics and equilibria of nucleosomes at elevated ionic strength, J. Biol. Chem. 259 (1984) 4212–4222.

[34] J. Ausió, D. Seger, H. Eisenberg, Nucleosome core particle stability and conformational change. Effect of temperature, particle and NaCl concentrations, and crosslinking of histone H3 sulfhydryl groups, J. Mol. Biol. 176 (1984) 77–104.

[35] J. Ausió, Y. Haik, D. Seger, H. Eisenberg, Histone-histone and histone-DNA interactions in chromatin, in: Sund, Veeger (Eds.), Mobility and Recognition in Cell Biology, Walter de Gruyter, Berlin, 1983, pp. 195–211.

[36] G. Voordouw, H. Eisenberg, Binding of additional histones to chromatin core particles, Nature 273 (1978) 446–448.

[37] K.J. Polach, J. Widom, Mechanism of protein access to specific DNA sequences in chromatin: a dynamic equilibrium model for gene regulation, J. Mol. Biol. 254 (1995) 130–149.

[38] G.S. Manning, The trajectory of a stiff rod in a curved potential energy trough. An initial result for short nucleosomal rods, Cell Biophys. 7 (1985) 177–184.

[39] N.L. Marky, G.S. Manning, The elastic resilience of DNA can induce all-or-none structural transitions in the nucleosome core particle, Biopolymers 31 (1991) 1543–1957.

[40] N.L. Marky, G.S. Manning, A theory of DNA dissociation from the nucleosome, J. Mol. Biol. 254 (1995) 50–61.

[41] N. Ramsay, G. Felsenfeld, B. Rushton, J.D. McGhee, A 145-base pair DNA sequence that positions itself precisely and asymmetrically on the nucleosome core, EMBO J. 3 (1984) 2605–2611.

[42] J.J. Hayes, K-M. Lee, In vitro reconstitution and analysis of mononucleosomes containing defined DNAs and proteins, Methods 12 (1997) 2–9.

[43] I. Isenberg, The cell nucleus, in: H. Busch (Ed.), Histones, 4, Academic Press, New York, 1978, pp. 135–154.

[44] D.E. Roark, Assaying histone interactions by sedimentation equilibrium and other methods, in: G. Stein, J. Stein, L.J. Kleinscmidt (Eds.), Methods in Cell Biology, 18, Academic Press, New York, 1978, pp. 417–428.

[45] D.E. Roark, T.E. Geoghegan, G.H. Keller, A two-subunit histone complex from calf thymus, Biochem. Biophys. Res. Commun. 59 (1974) 542–547.

[46] D.E. Roark, T.E. Geoghegan, G.H. Keller, K.V. Matter, R.L. Engle, Histone interactions in solution and susceptibility to denaturation, Biochemistry 15 (1976) 3019–3025.

[47] T.H. Eickbush, E.N. Moudrianakis, The histone core complex: an octamer assembled by two sets of protein-protein interactions, Biochemistry 17 (1978) 4955–4964.

[48] J.E. Godfrey, T.H. Eickbush, E.N. Moudrianakis, Reversible association of calf thymus histones to form the symmetrical octamer $(H2AH2BH3H4)_2$: a case of a mixed associating system, Biochemistry 19 (1980) 1339.

[49] G. Arents, R.W. Burlingame, B.-C. Wang, W.E. Love, E.N. Moudrianakis, The nucleosomal core histone octamer at 3.1 Å resolution: a tripartite protein assembly and a left-handed superhelix, Proc. Natl. Acad. Sci. USA 88 (1991) 10148–10152.

[50] J.O. Thomas, P.J.G. Butler, Size-dependence of a stable higher-order structure of chromatin, J. Mol. Biol. 144 (1980) 89–93.

[51] P.J.G. Butler, J.O. Thomas, Changes of chromatin folding in solution, J. Mol. Biol. 140 (1980) 505–529.

[52] J. Ausió, N. Borochov, D. Seger, H. Eisenberg, Interaction of chromatin with NaCl and $MgCl_2$. Solubility and binding studies, transition to and characterization of the higher-order structure, J. Mol. Biol. 177 (1984) 373–398.

[53] J. Ausió, N. Borochov, Z. Kam, M. Reich, D. Seger, H. Eisenberg, DNA conformation and folding from solution to higher order structure of chromatin, in: C. Helene (Ed.), Structure, Dynamics, Interactions and Evolution of Biological Macromolecules, D. Reidel Publishing, 1983, pp. 89–100.

[54] N. Borochov, J. Ausió, H. Eisenberg, Interaction and conformational changes of chromatin with divalent ions, Nucleic Acids Res. 12 (1984) 3089–3096.

[55] K.O. Greulich, J. Ausió, D. Seger, E. Wachtel, H. Eisenberg, Chromatin folding into higher-order structure, Biophys J. 49 (1986) 7–8.

[56] K.O. Greulich, E. Wachtel, J. Ausió, D. Seger, H. Eisenberg, Transition of chromatin from the '10 nm' lower order structure, to the '30 nm' higher order structure as followed by small angle X-ray scattering, J. Mol. Biol. 193 (1987) 709–721.

[57] K.O. Greulich, E. Wachtel, J. Ausió, D. Seger, H. Eisenberg, Transition of chromatin from the '10 nm' lower order structure, to the '30 nm' higher order structure as followed by small angle X-ray scattering, in: I. Chaiken, E. Chiacone, A. Fontana, R. Neri (Eds.), Macromolecular Recognition Principles and Methods, Humana Press, Clifton, NJ, 1987, pp. 153–168.

[58] J. Ausió, R. Sasi, G.D. Fasman, Biochemical and physiochemical characterization of chromatin fractions with different degrees of solubility isolated from chicken erythrocyte nuclei, Biochemistry 25 (1986) 1981–1988.

[59] M. García-Ramírez, F. Dong, J. Ausió, Role of the histone 'tails' in the folding of oligonucleosomes depleted of histone H1, J. Biol. Chem. 267 (1992) 19587–19595.

[60] S.H. Leuba, G. Yang, C. Robert et al., Three-dimensional structure of extended chromatin fibers as revealed by tapping-mode scanning force microscopy, Proc. Natl. Acad. USA 91 (1994) 11621–11625.

[61] J. Bednar, R.A. Horowitz, S.A. Grigoryev et al., Nucleosomes, linker DNA, and linker histone form a unique structural motif that directs the higher-order folding and compaction of chromatin, Proc. Natl. Acad. USA 95 (1998) 14173–14178.

[62] P.J. Butler, J.O. Thomas, Dinucleosomes show compaction by ionic strength, consistent with bending of linker DNA, J. Mol. Biol. 281 (1998) 401–407.

[63] F. Thoma, T. Keller, A. Klug, Involvement of histone H1 in the organization of the nucleosome and of the salt-dependent superstructures of chromatin, J. Cell Biol. 83 (1979) 403–427.

[64] K.E. van Holde, J. Zlanatova, What determines the folding of the chromatin fiber? Proc. Natl. Acad. Sci. USA 93 (1996) 10548–10555.

[65] V. Ramakrishnan, Histone H1 and chromatin higher-order structure, Crit. Rev. Eukaryotic Gene Expr. 7 (1997) 215–230.

[66] J. Allan, N. Harborne, D.C. Rau, H. Gould, Participation of core histone 'tails' in the stabilization of the chromatin solenoid, J. Cell Biol. 93 (1982) 285–297.

[67] M. García-Ramírez, C. Rocchini, J. Ausió, Modulation of chromatin folding by histone acetylation, J. Biol. Chem. 270 (1995) 17923–17928.

[68] S.C. Moore, M. Iskandar, J. Ausió, Major role of the histones H3-H4 in the folding of the chromatin fiber, Biochem. Biophys. Res. Commun. 230 (1997) 136–139.

[69] T.M. Fletcher, J.C. Hansen, The nucleosomal array: structure/function relationships, Crit. Rev. Eukaryotic Gene Expr. 6 (1996) 149–188.

[70] D.J. Clark, T. Kimura, Electrostatic mechanism of chromatin folding, J. Mol. Biol. 211 (1990) 883–896.

[71] H.K. Schachman, Analytical ultracentrifugation reborn, Nature 341 (1989) 259–260.

[72] T.M. Laue, Advances in sedimentation velocity analysis, Biophys. J. 72 (1997) 395–396.

[73] T. Simpson, F. Thoma, J.M. Brubaker, Chromatin reconstituted from tandemly repeated cloned DNA fragments and core histones: a model system for study of higher order structure, Cell 42 (1985) 799–808.

[74] J.C. Hansen, J. Ausió, V.H. Stanik, K.E. van Holde, Homogeneous reconstituted oligonucleosomes, evidence for salt-dependent folding in the absence of histone H1, Biochemistry 28 (1989) 9129–9136.

[75] J.G. Kirkwood, The general theory of irreversible processes in solutions of macromolecules, J. Pol. Sci. 12 (1954) 1–14.

[76] K.E. van Holde, Sedimentation analysis of proteins, in: R. Hill, H. Neurath (Eds.), Proteins, 3rd ed, I, Academic Press, San Francisco, 1975, pp. 225–291.

[77] L. Howe, M. Iskandar, J. Ausió, Folding of chromatin in the presence of heterogeneous H1 binding to nucleosomes, J. Biol. Chem. 273 (1998) 11625–11629.

[78] L.M. Carruthers, J. Bednar, C.W. Woodcock, J.C. Hansen, Linker histones stabilize the intrinsic salt-dependent folding of nucleosomal arrays: mechanistic ramifications for higher-order chromatin folding, Biochemistry 37 (1998) 14776–14787.

[79] J. Ausió, S.C. Moore, Reconstitution of chromatin complexes from high-performance liquid chromatography-purified histones, Methods 15 (1998) 333.

[80] S.C. Moore, P. Rice, M. Iskandar, J. Ausió, Reconstitution of native-like nucleosome core particles from reversed-phase-HPLC-fractionated histones, Biochem. J. 328 (1997) 409–414.

[81] A. Rabbani, M. Iskandar, J. Ausió, Daunomycin-induced unfolding and aggregation of chromatin, J. Biol. Chem. 274 (1999) 18401–18406.

[82] K. Tatchell, K.E. van Holde, Reconstitution of chromatin core particles, Biochemistry 16 (1977) 5295–5303.